International Journal of Bridge Engineering (IJBE), Vol. 1, No. 1, (2013), pp. 3-27

STATIC AND DYNAMIC NONLINEAR MODELLING OF LONG-SPAN CABLE-STAYED BRIDGES

Domenico Bruno[1], Fabrizio Greco[2], Paolo Lonetti[3],

[1,2,3] University of Calabria, Dept. of Civil Engineering, Italy
e-mail: domenico.bruno@unical.it, fabrizio.greco@unical.it, paolo.lonetti@unical.it

ABSTRACT: The aim of the paper is to provide numerical evaluations of the static and dynamic behavior of long span cable stayed bridges. In particular, investigations are presented to evaluate, in the framework of a dynamic analysis, the behavior of cable stayed bridges when subjected to the action of moving loads. In addition, the nonlinear static behavior is analyzed with the purpose to evaluate the influence of the geometrically nonlinear effects on the instability phenomena affecting the bridge structure. In both cases, the basic formulation is developed by using a finite element approach, in which a refined schematization is adopted to analyze the interaction behavior between cable system, girder and pylons. The proposed model takes into account geometrical nonlinearities of girder, pylons and of the cable system, for which local vibrations of the stays are also considered. Sensitivity analyses are proposed in terms of dynamic impact factors, emphasizing the effects produced by the external mass of the moving system and the influence of both "A" and "H" shaped tower typologies on the dynamic bridge behavior. Parametric results, developed in the framework of nonlinear static analysis, are also presented to evaluate the effects produced by instability effect of the axial compression in the girder on the maximum load-carrying capacity of the bridge.

KEYWORDS: Cable-stayed bridges, geometrical nonlinearities, instability, moving load effects, finite element model.

1 INTRODUCTION

Cable supported bridges have become an efficient solution for long span crossing, due to the notable progress in structural engineering, material and construction technologies [1]. As concerns long-span bridges, one of the most important problems is related to the deformability under live loads. As a matter of fact, long span cable-stayed bridges exhibit a remarkable nonlinear behavior under dead and live loads. Nonlinear effects in cable stayed bridges may arise from different sources. In particular, the cable system is affected by the nonlinear behavior of single elements, since they exhibit a different response in loading and in unloading due to the cable sag effect induced by self-weight.

Additional nonlinear effects may arise owing to changes in geometrical configurations due to large deflection effects (usually large rotations but small strains) in both towers and girder due to their slenderness, geometrical destabilizing effects of the axial compression induced in the towers and girder by the cable system [2, 3]. As a consequence, several studies have been carried out in the literature to analyze the nonlinear structural behavior of cable stayed bridges [2-9]. Some simplified assumptions have been introduced regarding the different sources of nonlinearities in most studies, in order to reduce the complexity of the highly non-linear problem. Due to its highly nonlinear behavior a standard analysis of the cable-stayed bridge, based on linear assumptions and on the tangent value of the equivalent elasticity modulus [6], may be not appropriate for long span bridges characterized by slender and lighter main girders [5, 1]. As a matter of fact, existing models based on the equivalent tangent modulus of elasticity or those assuming that the cable resists only tensile axial force with no stiffness against axial compression (tension only truss behavior), may lead to a notable underestimation of the maximum load carrying capacity of the bridge for specific loading conditions, since the softening behavior of the cable under unloading is not accurately represented.

Additional complexities may arise to investigate the behavior of long span bridges subjected to moving loads. In this context, the influence of mass distribution of the moving system, local vibration effects of the cable elements and the interaction between bridge and moving system kinematic are able to produce significant dynamic amplification effects in both displacement and stress bridge variables [10-14]. Moreover, due to new developments in the rapid transportation systems, the allowable speed range is significantly increased. As a consequence, non standard excitation modes determine extreme loading conditions, which, strongly, influence dynamic bridge behavior. To this aim, different investigations are needed to describe the interaction behavior between external moving system and bridge vibrations and, consequently, to accurately estimate dynamic impact factors of typical design bridge variables. The extension of the moving load problem for cable supported bridges with long spans requires a consistent approach to correctly analyze train-girder interaction. However, the references dealing with the dynamic response of cable supported bridges in the framework of moving loads are relatively few. For cable stayed systems, the effects produced by moving vehicles or railway loads have been analyzed, in terms of dynamic amplification factors related to both displacement or stress variables, with respect to bridges of reduced span only [15-17]. In the proposed work, the behavior of long span bridges is analyzed by using a generalized formulation based on the finite element method, in which both in plane and out-of plane deformation modes have been accounted for. Cable-stayed bridges based on both “H” and “A” shaped typologies with a double layer of stays have been considered. A parametric study in a dimensionless context has been analyzed by means of numerical results, in

terms of typical kinematic and stress bridge variables for both in plane and eccentric loading conditions. In particular, in the framework of the dynamic analysis, results are proposed to investigate the effects of moving system description with reference to non-standard forces due to Coriolis and centripetal accelerations, which are usually neglected in conventional dynamic analyses. Moreover, results developed in the framework of nonlinear static analysis are devoted to quantify the effects produced by instability phenomena in the bridge components on the on the maximum load-carrying capacity of the bridge.

2 CABLE-STAYED BRIDGE MODEL

In this section the governing equations for the bridge constituents as well as the main assumptions concerning the kinematic modeling are discussed. In particular, the main assumptions concerning the kinematic modeling of the bridge, the inertial forces to define the moving loads/girder interaction as well as those involved by the destabilizing effects produced in both girder and pylons are analyzed.

2.1 Formulation of the bridge model

The bridge scheme is based on a tridimensional modeling, in which both in plane and out of plane deformation modes are considered. The structural model, reported in Fig.1, is consistent with a fan-shaped and a self-anchored cable stayed bridge scheme. Moreover, the pylons refer to A or H-shaped typologies.

The cable kinematic is defined starting from the initial configuration under dead loads (DL), namely Ξ_0, whose details concerning the solving procedure are reported in Sec.2.2. The cable position vector, $\underset{\sim}{\varphi}$, due to the application of live loads is described by means of the following additive expression:

$$\underset{\sim}{\varphi}\left(\underset{\sim}{X},t\right) = \left(X_1^0 + U_1^C\left(\underset{\sim}{X},t\right)\right)\underset{\sim}{n}_1 + \left(X_2^0 + U_2^C\left(\underset{\sim}{X},t\right)\right)\underset{\sim}{n}_2 + \left(X_3^0 + U_3^C\left(\underset{\sim}{X},t\right)\right)\underset{\sim}{n}_3 \quad (1)$$

where the superscript $\cdot^0$ represents, here and in the following, variables associated to the initial configuration, $\underset{\sim}{X}$, with $\underset{\sim}{X}^T = \left[X_1, X_2, X_3\right]$, is the positional vector of the cable with respect to the reference system and U_i^C, with *i=1,2,3*, are the displacement components in the local reference system X_i described by the basis n_i of the coordinate system [18]. Moreover, the constitutive laws of the cable are defined by the second Piola-Kirchhoff stress S_1^C and Green-Lagrange strain E_1^C as follows:

$$S_1^C\left(\underset{\sim}{X},t\right) = S_0^C + C^C E_1^C\left(\underset{\sim}{X},t\right) \quad (2)$$

with

$$E_1^C\ \underset{\sim}{X},t\ = U_{1,X_1}^C\ \underset{\sim}{X},t\ + \frac{1}{2}\Big[U_{1,X_1}^2\ \underset{\sim}{X},t\ + U_{2,X_1}^2\ \underset{\sim}{X},t\ + U_{3,X_1}^2\ \underset{\sim}{X},t\ \Big]^C \quad (3)$$

where C^C is the elastic modulus, S_0^C is the stress referred to the initial configuration.

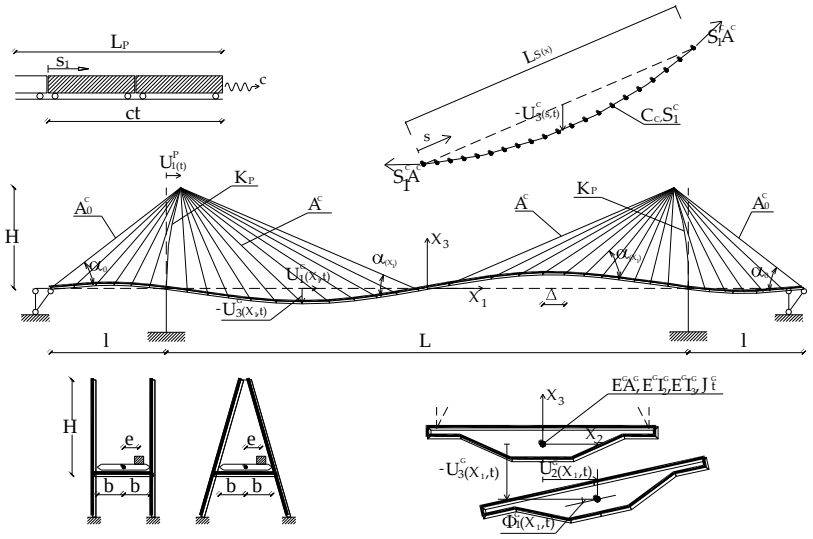

Figure.1. Cable stayed bridge scheme: bridge kinematic, pylon, girder and cable system characteristics.

Girder and towers are consistent with a beam model based on the Euler-Bernoulli formulation, in which large displacements are considered by using Green-Lagrange strain measure. Moreover, the torsional behavior owing to eccentric loading is described by means of the classical De Saint Venant theory. The displacements of the cross section for a generic point located at the X_1, X_2, X_3 coordinate, i.e. $\overline{U}_1^G, \overline{U}_2^G, \overline{U}_3^G$, are expressed by the following relationships:

$$\begin{aligned}
&\overline{U}_1^G\ X_1, X_2, X_3, t\ = U_1^G\ X_1, t\ + \Phi_2^G\ X_1, t\ X_3 - \Phi_3^G\ X_1, t\ X_2, \\
&\overline{U}_2^G\ X_1, t\ = U_2^G\ X_1, t\ , \\
&\overline{U}_3^G\ X_1, X_2, X_3, t\ = U_3^G\ X_1, t\ + \Phi_1^G\ X_1, t\ X_2
\end{aligned} \quad (4)$$

where U_1^G, U_2^G, U_3^G and $\Phi_1^G, \Phi_2^G, \Phi_3^G$ are the displacement and rotation fields

of the centroid axis of the girder with respect to the global reference system, respectively. The constitutive relationships are defined on the bases of moderately large rotations in which only the square of the terms U^{2G}_{i,X_1} representing the rotations of the transverse normal line in the beam are considered. Starting from the status concerning the initial configuration in which only dead loading are considered, the following relationships between generalized strain and stress variables are obtained:

$$\begin{aligned}
&N_1^G = N_1^{0(G)} + C^G A^G \varepsilon_1^G = N_1^{0(G)} + C^G A^G \left\{ U^G_{1,X_1} + \frac{1}{2}\left[U^{2\,G}_{1,X_1} + U^{2\,G}_{2,X_1} + U^{2\,G}_{3,X_1} \right] \right\}, \\
&M_2^G = M_2^{0(G)} + C^G I_2^G \chi_2^G = M_2^{0(G)} + C^G I_2^G \Phi^G_{2,X_1} = M_2^{0(G)} - C^G I_2^G U^G_{3,X_1 X_1}, \\
&M_3^G = M_3^{0(G)} + C^G I_3^G \chi_3^G = M_3^{0(G)} + C^G I_3^G \Phi^G_{3,X_1} = M_3^{0(G)} + C^G I_3^G U^G_{2,X_1 X_1}, \\
&M_1^G = G^G J_t^G \Theta^G = G^G J_t^G \Phi^G_{1,X_1},
\end{aligned} \tag{5}$$

where $C^G A^G$ and ε_1^G are the axial stiffness and strain, χ_2^G and χ_3^G or $C^G I_2^G$ and $C^G I_3^G$ are the curvatures or the bending stiffnesses with respect to the X_2 and X_3 axes, respectively, Θ^G and $G^G J_t^G$ are the torsional curvature and stiffness, respectively, N_1^G is the axial stress resultant, M_2^G and M_3^G are the bending moments with respect to the X_2 and X_3 axes, respectively, M_1^G and $G^G J_t^G$ are torsional moment and girder stiffness, respectively.

2.2 Initial configuration under dead loads

In order to analyze the actual behavior of the cable system the initial configuration in terms of stresses and strains should be determined. In particular, with reference to the cable-stayed bridge scheme, reported in Fig.2, with *n* number of stays, the objective functions are represented by the displacement vector $\underset{\sim}{U}$ containing the *n-2* vertical displacements, i.e. $U_2^G, ..., U_{n-3}^G, U_{n-2}^G$, excluding those points associated with the anchor stays at the cable/girder connections, and the horizontal displacements of the top cross section of the pylons (U_L^P, U_R^P):

$$\underset{\sim}{U}^T = \left[U_L^P, U_R^P, U_1^G, ..., U_{n-3}^G, U_{n-2}^G \right], \tag{6}$$

Moreover, the design variables, which have to be calculated, correspond to the internal stress distribution of the cable system, i.e. $\underset{\sim}{S}^T = \left[S_1^C, S_2^C, ..., S_{n_c-1}^C, S_n^C \right]$. Since the relationships between displacements and cable stresses are essentially nonlinear, a specialized solving procedure to calculate the initial configuration is required. In particular, starting from an initial trial distribution in the cable

system, i.e. $\underset{\sim}{S}_0$, the vertical displacements under the dead loading can be expressed to the first order by the Taylor expansion in terms of the incremental cable stress distribution, by means of the following linearized equation:

$$\underset{\sim}{U}\left(\underset{\sim}{S}_0+\Delta\underset{\sim}{S},g\right)=\underset{\sim}{U}\left(\underset{\sim}{S}_0,g\right)+\left.\frac{d\underset{\sim}{U}}{d\underset{\sim}{S}}\right|_{\underset{\sim}{S}_0,g}\cdot\Delta\underset{\sim}{S}+o\left\|\Delta\underset{\sim}{S}^2\right\| \tag{7}$$

where $\underset{\sim}{U}\left(\underset{\sim}{S}_0,g\right)$ is a vector containing the displacements in the self-weight loading condition and subjected to the stress distribution $\underset{\sim}{S}_0$, g is the loading parameter associated to the application of the dead loading and $\left.\frac{d\underset{\sim}{U}}{d\underset{\sim}{S}}\right|_{\underset{\sim}{S}_0,g}$ is the directional derivative of $\underset{\sim}{U}$ at $\underset{\sim}{S}_0$ coinciding with the flexibility matrix of the structure. In Eq.(7), the unknown quantity is represented by the incremental vector related to the cable stress distribution, namely $\Delta\underset{\sim}{S}$, which is determined enforcing the displacement vector $\underset{\sim}{U}\left(\underset{\sim}{S}+\Delta\underset{\sim}{S},g\right)$ to be zero under the action of the dead loading. Since the structure is affected by a nonlinear behavior, an iterative procedure based on the Newton-Raphson scheme is adopted. Moreover, the initial value of the stresses of a generic stay or the anchor stays are assumed to be equal to fixed working stress values, namely σ_g and σ_{g0} respectively, which are defined on the basis of the ratio between live load *p* and dead load *g*, the allowable stay stress and the geometric characteristics of the bridges, by means of the following relationships [19-21]

$$\sigma_g=\frac{g}{g+p}\sigma_a \qquad \sigma_{g0}=\sigma_a\left\{1+\frac{p}{g}[1-(\frac{2L}{l})^2]^{-1}\right\}^{-1}, \tag{8}$$

Similarly, the geometric measurement for the cables system can be expressed by the following equations [7-10, 31]:

$$A_i^C=\frac{g\Delta_i}{\sigma_g\sin\alpha_i}, \qquad A_0^C=\frac{gl}{2\sigma_{g0}}[1+(\frac{l}{H})^2]^{1/2}[(\frac{L}{2l})^2-1], \tag{9}$$

where α_i is the slope of a generic stay element with respect to the reference system, *(L,l,H)* are representative geometric lengths of the bridge structure, and Δ is the stay spacing step

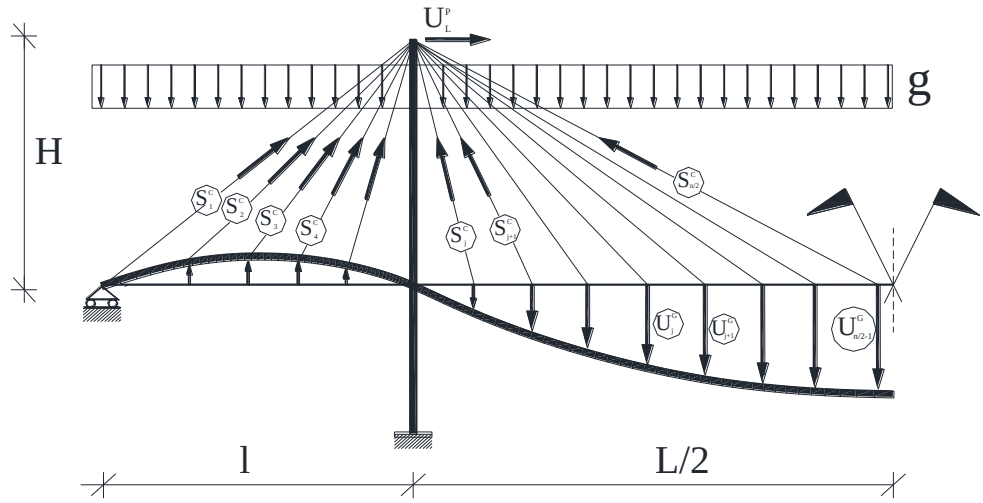

Figure.2. Cable stayed configuration under dead loading: definition of the internal stresses and kinematic parameters.

2.3 Nonlinear static bridge behaviour

An accurate determination of cable non-linear response within a nonlinear static analysis is compulsory in order to avoid inappropriate predictions of the actual load carrying capacity.

For large stress increments the secant modulus approach must be adopted in place of the tangent one, due to the high geometrical nonlinearity related to self-weight of the stay. Accordingly the stress increment in the stay $\Delta\sigma$ may be written in the form:

$$\Delta\sigma = E_s^* \ \Delta\varepsilon \ \Delta\varepsilon \,, \tag{10}$$

where E_s^* is the secant modulus of the stay a nonlinear function of the axial strain $\Delta\varepsilon$ (see Fig. 3).

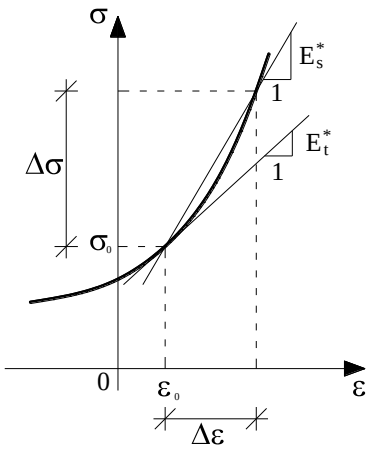

Figure.3. Stress-strain relationship of the cable.

For a parabolic approximation of the stay deformed configuration, the secant modulus has the following expression (see [1] for instance):

$$E_s^* = \frac{E}{1+\dfrac{\gamma^2 l_0^2 E}{12\sigma_0^3}\,\dfrac{1+\beta}{2\beta^2}}, \quad \beta = 1+\frac{\Delta\sigma}{\sigma_0}, \tag{11}$$

where E is the Young modulus, A the cable cross-sectional area, γ the cable weight per unit volume, l_o the horizontal projection of the stay length, and σ_0 the initial stress in the stay.

From Eq. (11) the tangent modulus expression ([5, 22]) can be obtained in the limit as the stress increments approaches zero from the initial configuration (i.e. $\beta \to 1$):

$$\frac{\Delta\sigma}{\Delta\varepsilon} = E_t^* = \lim_{\beta\to 1} E_s^* = \frac{E}{1+\dfrac{\gamma^2 l_0^2 E}{12\sigma_0^3}}. \tag{12}$$

The so-called tension only approximation can be obtained by assuming that when shortening occurs the cable stiffness vanishes (see for instance [1, 22]):

$$\frac{\Delta\sigma}{\Delta\varepsilon} = \begin{cases} E_t^* \;\; if \;\; \Delta\varepsilon \geq 0 \\ 0 \;\;\; if \;\; \Delta\varepsilon \leq 0 \end{cases}. \tag{13}$$

It must be evidenced that when the cable sag effect is neglected E_s^* can be replaced by E.
The different assumptions regarding the nonlinear cable response can be analyzed qualitatively with reference to a typical cable-stayed bridge scheme of fan shaped type, self-anchored with the girder not constrained in the horizontal direction and uniformly loaded on the central span. Assuming a simplified linear prebuckling behavior the girder's compression leads to equilibrium bifurcation when the load reaches its critical value. The postbuckling response depends on the shape of the buckling mode and may be affected by a decreasing behavior owing to the softening cable response in compression (see the dashed line curve in Fig. 4).
On the other hand the actual bridge behavior taking into account the nonlinear prebuckling effects, doesn't exhibit an equilibrium bifurcation as shown in continuous line in Fig. 4, and is similar to that of a structure with initial imperfections whose initial post-buckling behavior can be determined as a function of the idealized perfect structure. Owing to the softening behavior of the stress-strain stay relationship under shortening, a snap buckling behavior is expected with a local maximum in the static equilibrium path which can be significantly below the critical load.
The above described bridge behavior can be captured when the secant modulus model is adopted leading to a strong snap buckling behavior with a load maximum λ_{max} significantly below the critical load λ_c and with a post-buckling behavior of asymmetric unstable type. On the other hand, the tangent modulus approach leads to a non-conservative prediction since the corresponding limit load is larger than the one based on the secant modulus formulation. Moreover a mild snap buckling occurs as in a symmetric unstable bifurcation. It is worth noting that generally speaking the magnitude of the critical load, depending on the tangent modulus distribution along the stays, should changes slightly with respect to the secant modulus formulation.
On the contrary when the tension only truss model is adopted, the maximum load may be notably lower than the more accurate prediction obtained using the secant modulus model, thus giving a conservative prediction of the maximum load-carrying capacity.

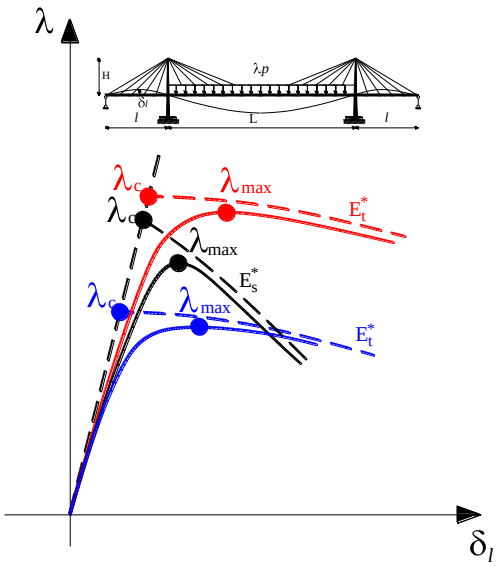

Figure. 4. Load parameter versus lateral midspan deflection curve.

2.4 Description of the moving load problem

The external loads are assumed to proceed, with constant speed *c* from left to right along the bridge development and are supposed to be located, eccentrically with respect to the geometric axis of the girder. The moving system description refers to railway vehicle loads, which are reproduced by means equivalent uniformly distributed loads, perfectly connected to the girder profile. As a result, the kinematic parameters of the moving system coincide with the ones defined by the girder, neglecting frictional forces arising from the external loads, roughness effects of the girder profile and local loading distribution produced by railway load components. However, these assumptions are quite recurrent in the framework of cable supported bridges with long spans, in which, typically, such interaction forces produced by localized dynamic effects are negligible with respect to the global bridge vibration [19]. Moreover, it is assumed that the damping energy is practically negligible. This hypothesis is verified in the context of long span bridges, where it has been proved that the bridge damping effects tend to decrease as span length increases [21]. With reference to the structural scheme reported in Fig.5, the infinitesimal reaction forces produced by the moving load on the girder profile can be expressed as a function of time dependent positional variable *s*, with $s\ t\ = ct$, by means of

the balance of linear momentum, as follows:

$$\begin{aligned} dR_{X_3} &= dX_1 \left\{ \lambda g + \frac{d\lambda}{dt}\frac{d\dot{\bar{U}}_3^m}{dt}\ s\ t\ + \lambda \frac{d^2\dot{\bar{U}}_3^m}{dt^2}\ s\ t\ \right\}\Bigg|_{s=X_1} \\ dR_{X_2} &= dX_1 \left\{ \frac{d\lambda}{dt}\frac{d\dot{\bar{U}}_2^m}{dt}\ s\ t\ + \lambda \frac{d^2\dot{\bar{U}}_2^m}{dt^2}\ s\ t\ \right\}\Bigg|_{s=X_1} \\ dR_{X_1} &= dX_1 \left\{ \frac{d\lambda}{dt}\frac{d\dot{\bar{U}}_1^m}{dt}\ s\ t\ + \lambda \frac{d^2\dot{\bar{U}}_1^m}{dt^2}\ s\ t\ \right\}\Bigg|_{s=X_1} \end{aligned} \tag{14}$$

where g is the gravitational acceleration, λ is the external mass per unit length and $\bar{U}_i^m$ with i=1,3 are the displacement functions along X_i axis of the moving mass, identified by the girder kinematic by using Eq.(4), as $\bar{U}_i^m = \bar{U}_i$. It is worth noting that in Eq.(14).1, at right hand side, the first term represents the dead loading contribution, whereas, the second term is produced by the unsteady mass distribution in the system due to time dependence character of the mass function arising from the moving loads. Finally, the third term must be calculated taking into account of the relative motion between bridge and the moving mass as follows [10]:

$$\frac{d\bar{U}_i^m}{dt} = \frac{\partial \bar{U}_i^m}{\partial t} + \frac{\partial \bar{U}_i^m}{\partial s}\frac{\partial s}{\partial t} = \frac{\partial \bar{U}_i^m}{\partial t} + \frac{\partial \bar{U}_i^m}{\partial s}c \tag{15}$$

$$\frac{d^2\bar{U}_i^m}{dt^2} = \frac{d}{dt}\left[\frac{\partial \bar{U}_i^m}{\partial t} + \frac{\partial \bar{U}_i^m}{\partial t}\frac{\partial s\ t}{\partial t} \right] = \frac{\partial^2 \bar{U}_i^m}{\partial t^2} + 2c\frac{\partial^2 \bar{U}_i^m}{\partial t \partial s} + c^2\frac{\partial^2 \bar{U}_i^m}{\partial s^2} \tag{16}$$

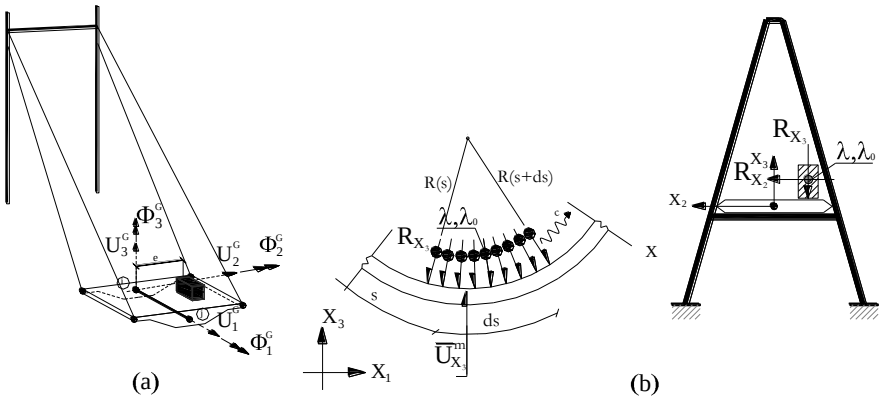

Figure.5. Girder kinematic (a) and moving loads description (b).

It is worth noting that the eulerian description of the moving system introduces in Eq.(16), three terms corresponding to standard, centripetal and Coriolis acceleration functions, respectively. However, the last two contributions in the acceleration function for the transverse and longitudinal displacements, i.e. when i=*1,2*, are typically negligible in comparison to the term associated with the standard acceleration and thus they are not considered in the following computations. Making the use of Eqs. (15)-(16), the reaction forces per unit length produced by the moving system are described by the following expressions:

$$p_{X_3} = \frac{dR_{X_3}}{dX_1} = \lambda g + \frac{d\lambda}{dt}\left[\left(\frac{\partial U_3^G}{\partial t} + e\frac{\partial \Phi_1^G}{\partial t}\right) + c\left(\frac{\partial U_3^G}{\partial X_1} + e\frac{\partial \Phi_1^G}{\partial X_1}\right)\right] + \\ + \lambda\left[\frac{\partial^2 U_3^G}{\partial t^2} + 2c\frac{\partial^2 U_3^G}{\partial t \partial X_1} + c\frac{\partial^2 U_3^G}{\partial X_1^{\,2}}\right] + \lambda \cdot e\left[\frac{\partial^2 \Phi_1^G}{\partial t^2} + 2c\frac{\partial^2 \Phi_1^G}{\partial t \partial X_1} + c\frac{\partial^2 \Phi_1^G}{\partial X_1^{\,2}}\right] \tag{17}$$

$$p_{X_2} = \frac{dR_{X_2}}{dX_1} = \frac{d\lambda}{dt}\frac{\partial U_2^G}{\partial t} + \lambda\frac{\partial^2 U_2^G}{\partial t^2} \tag{18}$$

$$p_{X_1} = \frac{dR_{X_1}}{dX_1} = \frac{d\lambda}{dt}\left[\left(\frac{\partial U_1^G}{\partial t} - e\frac{\partial \Phi_3^G}{\partial t}\right)\right] + \lambda\frac{\partial^2 U_1^G}{\partial t^2} - \lambda \cdot e\frac{\partial^2 \Phi_3^G}{\partial t^2} = \\ = \frac{d\lambda}{dt}\left[\left(\frac{\partial U_1^G}{\partial t} - e\frac{\partial^2 U_2^G}{\partial t \partial X_1}\right)\right] + \lambda\frac{\partial^2 U_1^G}{\partial t^2} - \lambda \cdot e\frac{\partial^3 U_3^G}{\partial t^2 \partial X_1} \tag{19}$$

where e is the eccentricity of the moving loads with respect to the girder geometric axis. Moreover, in Eqs. (17)-(19), the mass function during the external load advance can be expressed with respect to the global reference system assumed from the left end of the bridge as:

$$\lambda\ s_1, t\ = \lambda_{ML}\overline{H}\ s_1 + L_p - ct\ \overline{H}\ ct - s_1\ , \tag{20}$$

where $\overline{H}\ \cdot$ is the Heaviside step function, L_p is the length of the moving loads, s_1 is the referential coordinate located at the left end of the girder cross section, i.e. $s_1 = l + \frac{L}{2} + X_1$, and λ_{ML} is the mass linear density of the moving system.

3 FINITE ELEMENT FORMULATION

The cable system is modeled according to the multi element cable system approach, where each cable is discretized using multiple truss element and large deformations are accounted by using Green–Lagrange strains. The bridge has been modeled by means of a 3D assembly of non-linear beam elements and the

connections between cables and girder have been obtained by using constraint equations. This discrete model has been studied by means a displacement-type finite element (FE) approximation, implemented in the commercial software COMSOL MULTIPHYSICS TM [23]. In order to reduce the computational effort in the numerical calculations, a three dimensional finite element model has been developed by using beam elements for the girder and the pylons and nonlinear truss elements for the cable system. Specifically, the bridge deck is replaced by a longitudinal spline with equivalent sectional and material properties and the pylons are composed by two columns connected at their top and at the level of the bridge deck by two horizontal beam elements.
The destabilizing effects produced in both girder and pylons by the axial compression force induced by stays, has been accounted by adding the following weak contributions for the girder and pylons, respectively, to the virtual work principle formulation:

$$-\left(\int_{L_e} N_1^G \Phi_2 \delta\Phi_2 \, dL + \int_{L_e} N_1^G \Phi_3 \delta\Phi_3 \, dL \right),$$

$$-\left(\int_{L_e} N \Phi_2 \delta\Phi_2 \, dL + \int_{L_e} N \Phi_1 \delta\Phi_1 \, dL \right)$$

where N is the axial force, Φ_1, Φ_2, Φ_3 denote the bending rotation about the X_1, X_2, X_3 axes and L_e is the element length. The cable system is modeled according to the multi element cable system approach, according to which each cable is discretized using multiple truss element and the stiffness reduction caused by sagging is accounted for by allowing the cable to deform under applied loads. Large deformations are accounted by using Green–Lagrange strains and the axial strain is calculated by expressing the global strains in tangential derivatives and projecting the global strains on the cable edge. Additional details about the approach here adopted to model nonlinear cable behavior can be found in [23]. The tension only behavior is modeled by multiplying the longitudinal modulus of the truss element by a step function depending on the axial strain increment with respect to the initial configuration of the bridge under dead loading, in order to exclude any stiffness contribution of the cable under shortening. The constraint conditions between the girder and the stays are modeled with offset rigid links to accommodate cable anchor points by means of the extrusion coupling variable technique (see [23] for additional details).

Governing equations introduce a non linear set of equations, which have been solved numerically, using a user customized finite element program, i.e. COMSOL Multiphysics TM version 4.1 [23]. Finite element expressions are written starting from the weak form, introducing the interpolation functions ζ_i, ξ_i to represent cable (C) and girder/pylon (G,P) variables as:

$$\underset{\sim}{U}^{C}\ r,t\ =\sum_{i=1}^{n}\zeta_i\ \underset{\sim}{r}\ \underset{\sim}{u}_i^{C}\ t\ ,\ \underset{\sim}{U}^{G,P}\ r,t\ =\sum_{i=1}^{n}\xi_i\ \underset{\sim}{r}\ \underset{\sim}{u}_i^{G,P}\ t\ , \tag{21}$$

where n represents the number of nodes of the master finite element. In particular, Lagrange interpolation functions are adopted to analyze the behavior of the cable system, whereas for girder elements based on EB formulation Hermit cubic interpolation functions are employed.

The bucking and post-bucking behaviors have been investigated by using a solution strategy based on the damped Newton method has been adopted. An algebraic equation that controls the applied live loads λp so that the generalized deflection of a control point reaches the prescribed values, is introduced in the FE model by means of the ODE interface. Moreover, in order to capture the typical snapping behavior of the load-displacement curve, a generalized deflection increasing monotonically with the evolution of the loading process is chosen. For instance in the case of loading on the central span of the bridge, an appropriate choose to capture the snapping behavior is the lateral midspan deflection δ_l or the girder end in-plane rotation θ_l, although in some cases relevant to the tension only (TO model) the central midspan deflection δ_c has been adopted. For the dynamic analyses, in order to solve the nonlinear algebraic equations an implicit time integration scheme based on a variable step-size backward differentiation formula (BDF) is adopted. Moreover, during the time integration, due to the fast speeds of the moving loads, a small time step size is utilized, which typically, no more than 1/50 of the fundamental period of vibration of the structure.

4 RESULTS AND DISCUSSION

4.1 Static analysis: influence of nonlinear effects on the bridge behaviour

Numerical results devoted to the non-linear bridge response are presented in the following sections to analyze the influence of different loading conditions, geometrical configurations and pylon shapes. In the finite element model of the bridge both the H-type and A-type pylon shapes are analyzed and different eccentricities with respect to the deck axis of the live load are taken into account. In addition, two types of loading conditions are considered: a uniform load distributed on the whole bridge length and a uniform load applied on the central span only. In the numerical tests the following dimensionless parameters are adopted:

$$\frac{L}{2H}=2.5,\frac{l}{H}=5/3,\frac{b}{H}=0.1,\frac{\Delta}{L}=1/105,\frac{\sigma_a}{E}=7200/2.1\times10^6,\frac{K}{g}=50\,.$$

The value adopted for the dead load g is equal to 300,000 N/m, typical of a steel deck, whereas the cable unit volume weight has been assumed equal to

γ=77.01kN/m^3. The parameters ε, ε_A and a are used to define the bridge geometrical parameters according to the following formulas:

$$H = \sqrt{\frac{12a\sigma_g^3}{\gamma^2 E}},\ I = \frac{\varepsilon^4 H^3 g}{4\sigma_g},\ A = \frac{\varepsilon_A H g}{\sigma_g}.$$

Taking into account the previous parameters a parametric analysis is carried out for the bridge by adopting the following values for the above quantities: ε = 0.2 or 0.3, a = 0.10 or 0.20 and p/g = 0.5 or 1, whereas ε_A has been assumed equal to 54.5. Moreover, the following additional parameters are used to define the bending stiffness I_{zz} and the pylon bending stiffness $I_{p\,yy}$:

$$\varepsilon_h = \sqrt[4]{\frac{4I_{zz}\sigma_g}{b^3 g}},\ I_r = \frac{I_{p\,yy}}{I}.$$

The towers stiffness $I_{p\,xx}$ for out-of-plane bending has been assumed equal to $I_{p\,yy}$. The axial, bending and torsional stiffnesses of the beams connecting the two towers of the pylons have been assumed equal to the corresponding ones adopted for the towers. The cross section area and the torsional stiffness of the towers have been assumed equal to those of the girder. With reference to the above parameters additional analyses will be carried out in terms of I_r and ξ by adopting the following ranges of variation: ξ = 0 ÷ 0.5, I_r = 0.5 ÷ 70, while the following parameters have been assumed for the remaining parameters: τ=0.1, ε_h=5, t=0.1. In this section the influence of the different approaches which can be used to model the stays mechanical behavior on the bridge nonlinear response is analyzed by means of the general 3D finite element model introduced. In particular, the behavior of a single cable has been modeled by using the multiple truss element nonlinear formulation, which will be denoted as NLM, the tangent modulus linear model (denoted as LM) which adopts the initial stress derived from the initial shape analysis and the tension only approximation (denoted as TO).

The classical snapping for high values of the load parameter λ, due to the coupling between the softening behavior of cables response in the lateral span and the instabilizing effect of the axial compression in the girder, occurring in the case of the central loading condition and the H pylon shape, is presented in the Fig. 6, for ε=0.2 and 0.3, a=0.2 and p/g=0.5. As λ increases, while in the central span the instabilizing effect of the axial compression is balanced by the stiffening stays, in the lateral spans a large stress reduction occurs owing to the lateral spans deflection. Therefore an instability condition is reached, producing a bound in the applied load. The bridge deformed shape for the NLM model with ε=0.2, corresponding to the maximum load parameter, is illustrated in Fig. 7, by using a color map of the displacements. In Fig. 1 the results obtained by using the linear tangent model (LM) and the tension only model (TO), are also represented.

With reference to the actual behavior of the bridge (NLM), the load displacement curves, for different girder stiffness parameters, show a notable overestimation for the LM approach whereas an underestimation for the TO one. The results of parametric analyses for different values of the parameters ε, a and p/g are summarized only in terms of the maximum load parameter in Table 1, for both H and A pylon shape. These results show the strong stabilizing effect of the girder stiffness independently and confirm the considerations made on the basis of the load-displacement plotted of Fig. 6 about the overestimation of the LM one. The effect of the stay deformability parameter a is weaker than that of the girder stiffness one. Results show also how the pylon shape scarcely influences the non-linear static behavior of the bridge. Since the A pylon shape involves larger lengths in the cable system, the bridge deformability increases and this causes a small reduction of the maximum load parameter λ_{max} with respect to the H pylon shape.

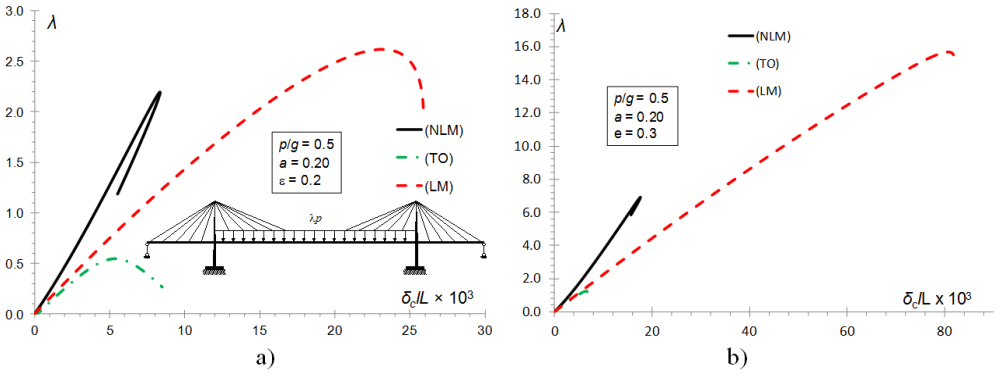

Figure 6. Load parameter λ versus central midspan deflection δc for the uniform loading condition and H pylon shape: ε=0.2 (a) and ε =0.3 (b).

Figure 7. Bridge deformed shape for the maximum load parameter for the NLM model of Fig. 6a.

	ε \ a	0.10				0.20			
		NLM (H)	LM (H)	NLM (A)	LM (A)	NLM (H)	LM (H)	NLM (A)	LM (A)
p/g =0.5	0.2	2.403	3.047	2.393	3.021	2.197	2.617	2.188	2.599
	0.3	7.109	14.156	7.065	14.005	6.910	15.669	6.865	15.464
p/g = 1	0.2	1.678	2.248	1.673	2.237	1.563	1.962	1.557	1.950
	0.3	4.476	9.918	4.450	9.813	4.380	11.534	4.353	11.377

Table 1. Influence of ε, a and p/g on λmax for the nonlinear (NLM), linear (LM) and tension-only (TO) approaches. Central loading condition.

In the case of the uniform loading the typical snap buckling behavior of the bridge is shown in Fig.8. For this loading condition the nonlinear behavior is governed by the instability effect of axial compression, while cables provide a stiffening effect except for a very small group of cables in the lateral span near the maximum load. The influence of the softening cable behavior under shortening is less appreciable with respect to the central loading case and the maximum load depends strictly on the nonlinear prebuckling effects which lead to larger displacements and rotations in the central span when the tangent modulus or the tension-only models are adopted.
The associated bridge deformed shape for the NLM model with ε=0.2 is illustrated in Fig. 9, corresponding to the maximum load parameter. The results obtained by using the linear tangent model (LM) and the tension only model (TO) are shown also in this case in order to appreciate the influence of the nonlinear cable response modeling on the global bridge behavior (see Fig. 8). Figure 8 shows how the LM and TO models are characterized by the same behavior, due to the fact that in the case of the uniform loading condition cables are always in tension except for a very small group of stays in the lateral span near the maximum load. Moreover, in this case it is possible to appreciate the conservative behavior of the LM and TO models with respect to the NLM, in terms of the maximum load parameter λ_{max}.
Also in this case, the results of parametric analyses carried out for different values of the parameters *ε, a* and *p/g*, are shown in Table 2 in terms of the maximum load parameter and for both H and A pylon shape. It can be evidenced that for all the analyzed models increasing the stay deformability parameter *a* leads to a reduction of the limit load, although the effect of this parameter appears notably weaker than that of the girder stiffness one.

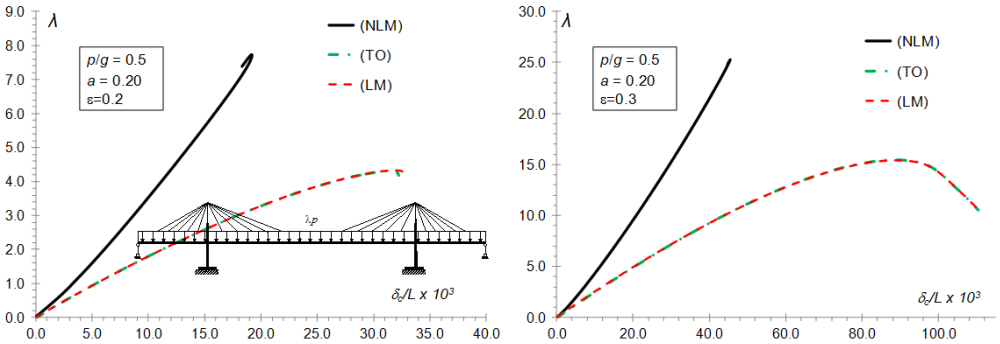

Figure 8. Load parameter λ versus δc (central midspan deflection) for the uniform loading condition and H pylon shape: ε=0.2(a) and ε =0.3(b).

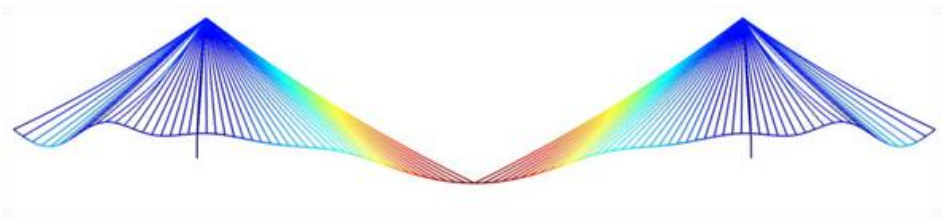

Fig. 9. Bridge deformed shape corresponding to the maximum load parameter for the NLM model in Fig. 8a.

	a / ε	0.10				0.20			
		NLM (H)	LM (H)	NLM (A)	LM (A)	NLM (H)	LM (H)	NLM (A)	LM (A)
p/g = 0.5	0.2	7.848	5.305	7.819	5.275	7.731	4.320	7.702	4.291
	0.3	25.315	16.376	25.188	16.274	25.244	15.439	25.115	15.338
p/g = 1	0.2	5.589	3.838	5.570	3.817	5.544	3.146	5.525	3.126
	0.3	17.077	11.391	16.994	11.322	17.068	11.332	17.020	11.180

Table 2. Influence of the parameters ε, a and p/g on the maximum load parameter λmax for the nonlinear (NLM), linear (LM) and tension-only (TO) approaches. Uniform loading condition.

The influence of the tower to girder bending stiffness ratio I_r on the maximum load parameter for the H pylon shape and different load eccentricity values e_c

are then analyzed, for a given live to dead load ratio (p/g = 1), a = 0.1 and ε = 0.2.

The plot of the maximum load parameter λ_{max} versus the tower to girder bending stiffness ratio I_r is presented, for the central loading condition, in Fig. 10a. Increasing I_r leads to an increment of the maximum load parameter since the prebuckling configuration involves smaller deflections and the associated prebuckling behavior can be considered as linear. The effects of load eccentricity are appreciable only for I_r less than 5, for which increasing load eccentricity leads to a transition from an in plane buckling to an out of plane buckling coupling pylons and girder.

In Fig. 10b the influence of the tower to girder stiffness ratio, in the case of uniform loading condition on the whole bridge length and for the H pylon shape, is represented. In particular, for uniform load applied on the entire bridge deck the load maximum level is more than three times respect to central load. The effect of load eccentricity is larger respect to the central loading case, whereas also in this case pylon buckling occurs for small values of I_r.

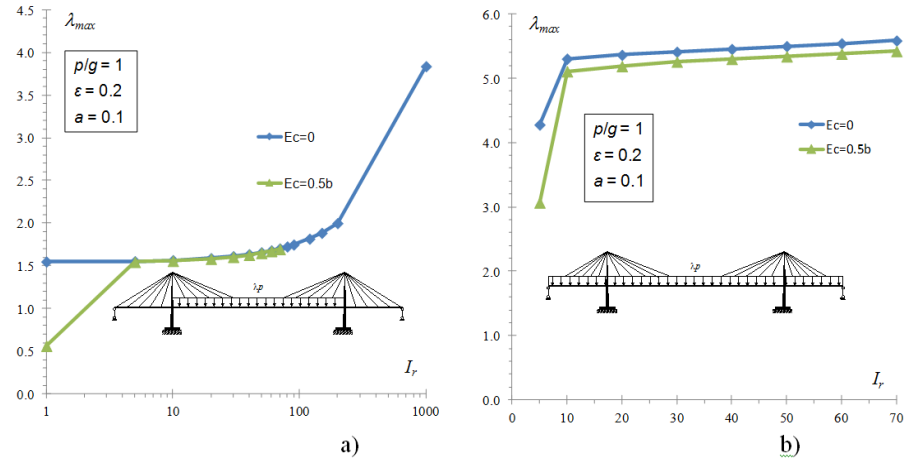

Figure 10. Effect of pylon bending stiffness and of load eccentricity on the maximum load parameter for H pylon shape: central loading condition (a) and uniform loading condition (b).

4.2 Dynamic analysis: effect of the moving loads.

The bridge and moving loads dimensioning has been opportunely selected consistently to typical values utilized in several bridge applications and mainly derived from both structural and economical reasons. As a result, the dimensionless parameters related to aspect ratio, pylon stiffness, allowable cable stress, moving loads characteristics are assumed equal to the following representative values [1,19-20]:

$$\frac{L}{2H}=2.5,\ \frac{\mathrm{l}}{H}=5/3,\ \frac{\mathrm{K_p}}{\mathrm{g}}=50,\zeta\ =\frac{\lambda}{\mu}=1,\ \zeta_0=\frac{\mu_0}{\mu b^2}=1.16,\tau_0=\frac{\lambda_0}{\lambda e^2}=1,$$

$$\varepsilon_{Fy,z}=\left(\frac{4I^G_{y,z}\sigma_g}{H^3 g}\right)^{1/4}=\ 0.2,0.48\ ,\ \varepsilon_\omega=\left(\frac{C_t\sigma_g}{Eb^2Hg}\right)^{1/2}=0.15, \tag{22}$$

$$\varepsilon_A=\left(\frac{A^G\sigma_g}{Hg}\right)=54.5,\ a=\left(\frac{\gamma^2H^2E}{12\sigma_g^3}\right)=0.1,\vartheta=c\left(\frac{\mu\sigma_g}{EgH}\right)^{1/2}$$

where σ_g is the design stress under self-weight loads, γ is the stays specific weight, C_t torsional girder stiffness, b is half girder width, e is the eccentricity of the moving loads with respect to the girder geometric axis and μ is the mass density of the girder, μ_0 and λ_0 are the torsional polar mass moment of the girder and moving load, respectively. The initial configuration is obtained assuming a proper erection procedure, which produces traction and compression states in cable system and girder/pylons, respectively. Comparisons have been proposed in terms of moving loads schematization, bridge size parameter, a, and girder stiffness properties for typical stress and kinematic design bridge variables. The parametric study provides an useful tool to estimate dynamic amplification factor dependence from both moving loads and bridge properties. The following kinematic and stress variables representative of the bridge behavior have been analyzed:

- $\phi_{V\ L/2}$ dynamic impact factor of the midspan vertical displacement,
- $\phi_{M\ L/2}$ dynamic impact factor of the midspan bending moment,
- ϕ_{σ_0} dynamic impact factor of the axial force in the anchor stay,
- ϕ_σ dynamic impact factor of the axial force in the longest central span stay.

The dimensionless parameters related to aspect ratio, pylon stiffness, allowable cable stress, moving loads characteristics, are assumed consistently with well-known design ranges and equal to the following representative values:

$$\mathrm{L/2H=2.5,\ l/H=5/3,\ \sigma_a/E=7200/2.1x10^6,\ K_p/g=50,\ p/g=[1,0.5]}, \tag{23}$$

In Figs.11a-b, comparisons in terms of dynamic impact factors are proposed, in which the influence of external loading with respect to a different external mass schematization has been evaluated. As a matter of this fact, the inertial effects produced by the moving mass are assumed at first to be completely neglected, i.e. λ=0, or evaluated with respect to both standard acceleration contribution only (no Coriolis, Centripetal acceleration terms) and for a steady mass

distribution of the global system formed by bridge and moving loads (namely, SA). The comparisons denote different predictions for high range of speed parameters between SA and proposed results, in which non-standard acceleration terms appear to provide notable amplifications in both kinematic and stress variables. Moreover, the proposed solution does not agree for low range of the speed parameter with the corresponding one in which the inertial effects are completely neglected, determining a notable underestimation in dynamic impact factors prediction.

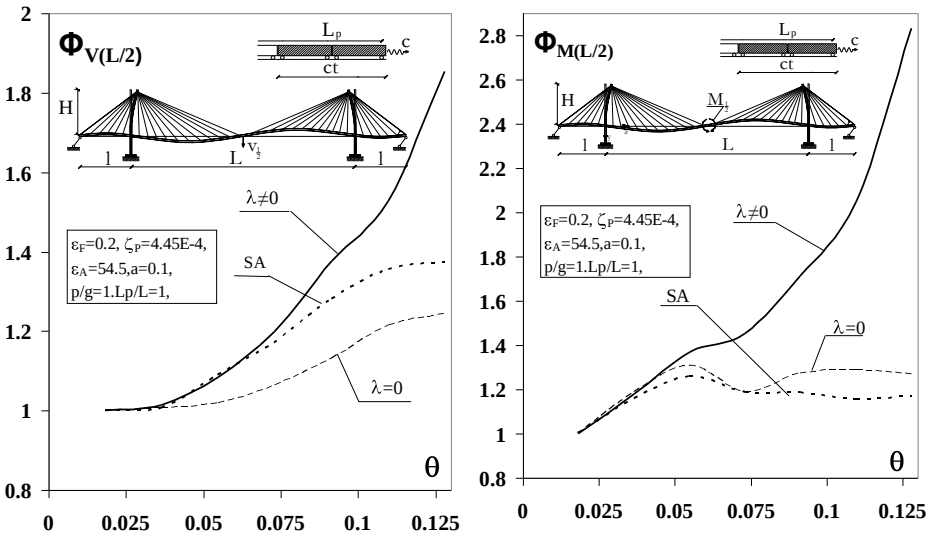

Figure 11a-b. Cable stayed system: vertical displacement and bending moment D. A. F. vs speed parameter

In Fig.12, at constant vehicle transit speed, the relationship between dynamic amplification factors and cable system efficiency is investigated. Therefore, in typically allowable ranges of the bridge size parameter *a*, commonly utilized in practical applications, dynamic impact factors related to kinematic (a) and stress (b) bridge quantities have been evaluated. The analyses have been developed for different lengths of the external transit loads. Furthermore, comparisons in terms of the moving mass characteristics have been proposed. The results show that inertial effects produce major amplifications in both displacement and stress variables, especially, for low values of bridge parameter *a*, in which the bridge structures is more influenced by the dynamic amplification effects. Finally, the results are quite dependent from the external mass schematization, because notable underestimations in both stress and displacement dynamic amplification factors have been noted, if the inertial effects produced by the moving loads have not properly accounted for.

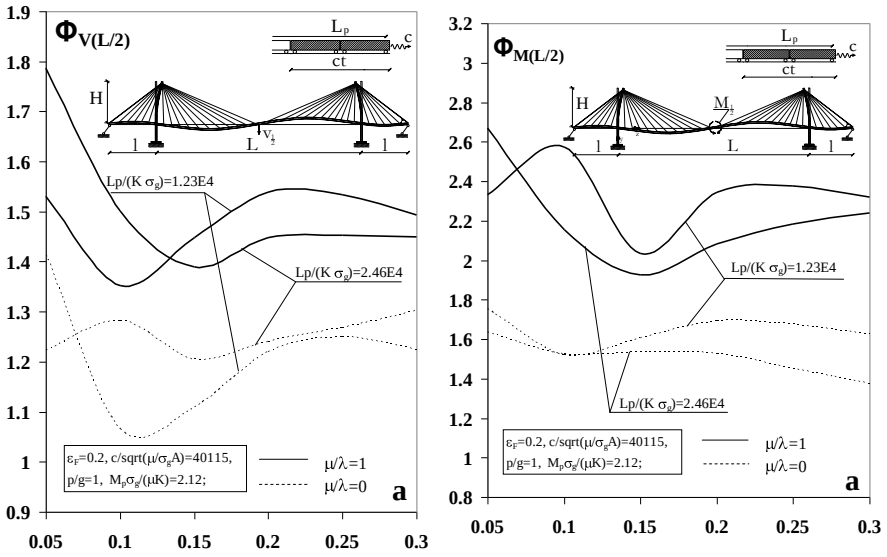

Figure 12a-b. Cable stayed system: mid span displacement and bending moment D. A. F. vs a parameter.

In Fig.13, sensitivity analyses in terms of the relative flexural stiffness parameter ε_f, have been proposed, emphasizing the effects produced by the external moving mass. The investigation has been developed for a moving load with speed and for different values of cable system efficiency ($a=0.1\div0.2$). The results display decreasing values of the amplification factors for increasing values of the ε_f stiffness parameter, whereas dynamic bridge behavior appears to be quite sensitive to the external mass schematization. The major amplification effects are noted for low ranges of ε_f parameter, in which the bridge structure is basically more flexible and mainly dominated by the cable system. Finally, in Fig.s 14, the effects of the eccentricity of the moving system for both A-shaped tower (AST) or H-shaped tower (HST) is investigated. In particular, comparisons to emphasize the prediction of the dynamic amplification factor and the maximum value of the torsional rotation, assuming different formulations in the prediction of cable suspension system behavior are developed (Fig.14a). Finally, in Fig.14-b, time histories of the vertical displacements related to different cross-sections of the longest cable of the suspension system are reported. The results show how the cable elements are subjected during the moving load application to an oscillating behavior in the vertical displacements, leading to local vibration effects along longitudinal axis of the stay.

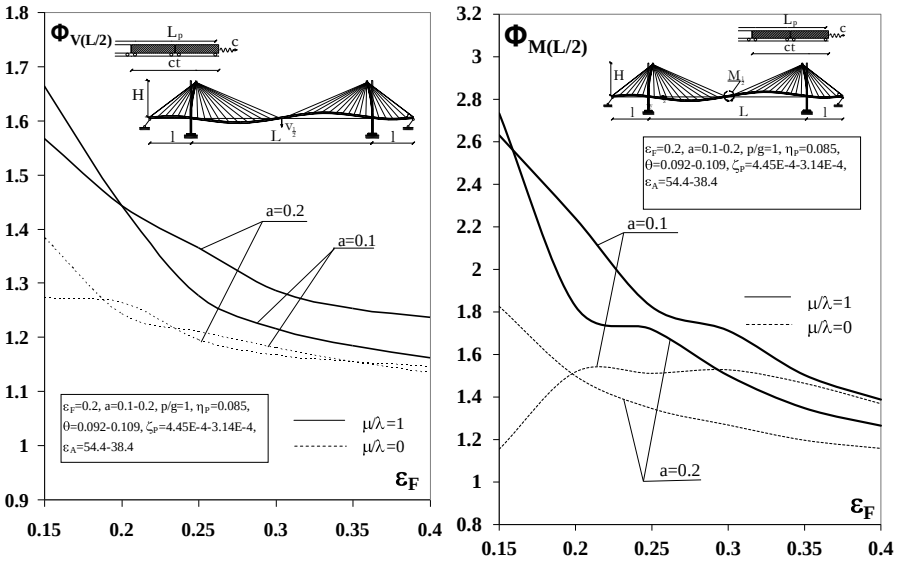

Figure 13a-b. Cable stayed system: midspan displacement and bending moment D. A. F. vs ε_f parameter.

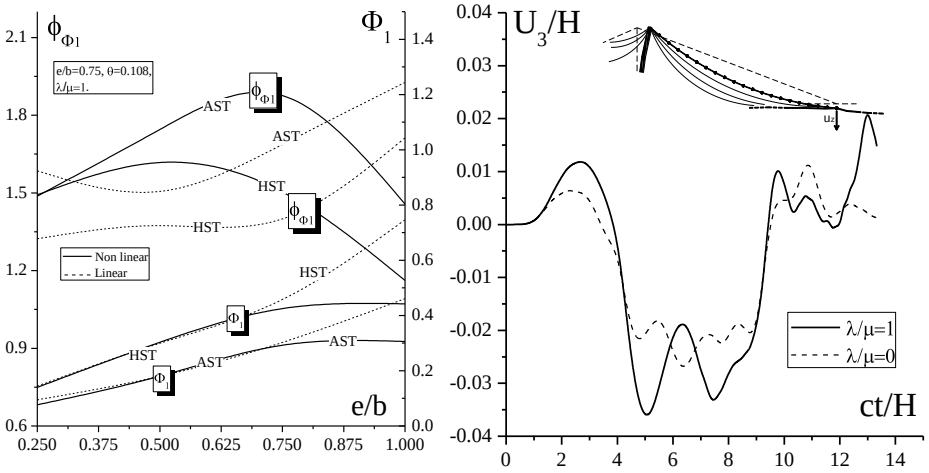

Figure 14a-b Midspan torsional rotation dynamic amplification factors and maximum displacement vs normalize eccentricity of the moving loads (e/b) for AST-HST (a). Time history of the vertical displacement of the longest stay (b)

CONCLUSIONS

Results obtained for the static non-linear behavior of the bridge show the strong influence of the nonlinear stays response in coupling with the instability effect of axial compression in girder and pylons, on the stability behavior of the

bridge. As a matter of fact, neglecting the nonlinear stays response leads to a notable overestimation of the actual loading carrying capacity of the bridge especially when the assumed loading condition produces cable unloading. On the other hand, other parameters such as pylon shape and stiffness and live load eccentricity may be less important factors in non-linear analysis. Moreover, the effects of the inertial description of the moving system on the dynamic bridge behavior have been investigated, by means of a parametric study developed in terms of both moving loads and bridge characteristics. The analyses have shown how the actual behavior of the bridges is quite influenced by mass description of the moving loads or the formulation adopted to analyze cable vibrations of the suspension system, leading to high dynamic amplification effects on typical stress or displacement design bridge variables.

REFERENCES

[1] Gimsing NJ. Cable supported bridges: concepts and design. New York: John Wiley & Sons Ltd; 1997

[2] Wang, P.H., Yang, C.G., "Parametric studies on cable-stayed bridges", Comput Struct, Vol. 60(2), pp. 243-260, 1996.

[3] Tang, C.C., Shu, H. S, Wang, Y.C., "Stability analysis of steel cable-stayed bridges" Structural Engineering and Mechanics, Vol., 11, pp. 35-48, 2001.

[4] Adeli, H., Zhang, J., "Fully nonlinear analysis of composite girder cable-stayed bridges" Comput Struct, Vol. 54(2), pp. 267–277. 1995.

[5] Bruno, D., Grimaldi, A. "Nonlinear behavior of long- span cable-stayed bridges", Meccanica, Vol. 20, pp.303-313, 1985.

[6] Fleming, J.F. "Nonlinear static analysis of cable-stayed bridge structures" Comput Struct, Vol. 10(4), pp. 621-635, 1979.

[7] Ying, X., Kuang, J.S. "Ultimate load capacity of cable-stayed bridges", Journal of Bridge Engineering, Vol. 4(1), 1999.

[8] Bruno D., Greco F., Nevone Blasi P., Bianchi, E. "A 3D nonlinear static analysis of long-span cable stayed bridges", Annals of Solid and Structural Mechanics, Vol. 5, Issue 1-2, pp. 15-34, 2013.

[9] Huu-Tai, T., Seung-Eock, K. "Nonlinear static and dynamic analysis of cable structures" Finite Elements in Analysis and Design, Vol. 47, pp. 237-246, 2011.

[10] Fryba L.. Vibration of solids and structures under moving loads. London: Thomas Telford; 1999.

[11] Warnitchai P., Fujino Y., Susumpow T. "A non-linear dynamic model for cables and its application to a cable-structure system". Journal of Sound and Vibration, Vol. 187, pp. 695-712, 1995.

[12] Warburton GB. The dynamical behavior of Structures, Oxford: Pergamon, 1976.

[13] Lei X, Noda NA. Analyses of dynamic "Response of vehicle and track coupling system with random irregularity of track vertical profile". Journal of Sound and Vibration, Vol. 258, pp. 147-165, 2002.

[14] Wiriyachai A, Chu KH, Garg VK. "Bridge impact due to wheel and track irregularities". J of Eng.rg Mech Div, Vol.108, pp. 648-665, 1982.

[15] Au FTK, Wang, JJ, Cheung, YK. "Impact study of cable-stayed bridge under railway traffic using various models". Journal of Sound and Vibration. Vol. 240, pp. 447-465, 2001.

[16] Au FTK, Wang, JJ, Cheung, YK. "Impact study of cable-stayed railway bridges with random rail irregularities". Engineering Structures.; Vol.24, pp.529-541, 2001.
[17] Yang F, Fonder GA. "Dynamic Response of Cable-Stayed Bridges under Moving Loads", J Engrg Mech.Vol.124, pp. 741-747, 1998.
[18] Wriggers P.. Nonlinear Finite Element Methods. Berlin: Springer-Verlag; 2008.
[19] Bruno, D., Greco, F., Lonetti, P. "Dynamic impact analysis of long span cable-stayed bridges under moving loads. Engineering Structures". Vol.30, pp. 1160-1177, 2008.
[20] Bruno D., Greco F., Lonetti P. "A parametric study on the dynamic behaviour of combined cable-stayed and suspension bridges under moving loads". International Journal for Computational Methods in Engineering Science & Mechanics. Vol. 10, pp. 243-258., 2009.
[21] Xia H., Xu Y.L., Chan T.H.T. "Dynamic interaction of long suspension bridges with running trains". Journal of Sound and Vibration. Vol.237, pp.263-280, 2000.
[22] Wang, P.-H., Lin, H.-T., Tang, T.-Y. "Study on nonlinear analysis of a highly redundant cable-stayed bridge" Computers and Structures, Vol. 80, pp. 165-182, 2002.
[23] COMSOL AB (September 2008) Structural Mechanics Module User's Guide.

Received: Dec. 20, 2013 Accepted: Dec. 28, 2013